Received: 10 August 2020 | Revised: 2 October 2020 | Accepted: 14 October 2020

DOI: 10.1111/liv.14706

ORIGINAL ARTICLE

Liver INTERNATIONAL WILEY

Qualification of tumour mutational burden by targeted next-generation sequencing as a biomarker in hepatocellular carcinoma

Ching Ngar Wong[1] | Petros Fessas[1] | Kathy Dominy[2] | Francesco A. Mauri[1] | Takahiro Kaneko[1,3] | Persephone Du Parcq[2] | Jamshid Khorashad[2] | Pierluigi Toniutto[4] | Robert D. Goldin[5] | Claudio Avellini[6] | David J. Pinato[1]

[1]Department of Surgery & Cancer, Imperial College London, Hammersmith Hospital, London, UK

[2]Molecular Pathology Laboratory, Hammersmith Hospital, London, UK

[3]Tokyo Medical and Dental University, Tokyo, Japan

[4]Hepatology and Liver Transplantation Unit, Department of Medical Area (DAME), University of Udine, Udine, Italy

[5]Centre for Pathology, Imperial College London, London, UK

[6]Azienda Ospedaliero-Universitaria "Santa Maria della Misericordia", Institute of Histopathology, Udine, Italy

Correspondence
David J. Pinato, Clinical Senior Lecturer and Consultant in Medical Oncology, Imperial College London Hammersmith Campus, Du Cane Road, W120 HS London, UK.
Email: david.pinato@imperial.ac.uk

Funding information
DJP is supported by grant funding from the Wellcome Trust Strategic Fund (PS3416) and by a Cancer Research UK Grant for the immune phenotyping of HCC (Postdoctoral Bursary Grant Ref. C57701/A26137).

Abstract

Background & Aims: Tumour mutational burden (TMB) predicts improved response and survival to immunotherapy. In this pilot study, we optimized targeted next-generation sequencing (tNGS) to estimate TMB in hepatocellular carcinoma (HCC).

Methods: We sequenced 48 non-paired samples (21 fresh-frozen [FF] and 27 paraffin-embedded [FFPE]), among which 11 FFPE samples were pretreated with uracil-DNA glycosylase (UDG). Thirty samples satisfied post-sequencing quality control. High/low TMB was defined by median number of mutations/Mb (Mut/Mb), across different minimum allele frequency (MAF) thresholds (≥0.05, ≥0.1 and ≥0.2).

Results: Eligible patients (n = 29) were cirrhotic (84%) with TNM stage I-II HCC (75%). FFPE samples had higher TMB (median 958.39 vs 2.51 Mut/Mb, $P < .0001$), estimated deamination counts (median 1335.50 vs 0, $P < .0001$) and C > T transitions at CpG sites (median 60.3% vs 9.1%, $P = .002$) compared to FF. UDG-treated samples had lower TMB (median 4019.92 vs 353 Mut/Mb, $P = .041$) and deamination counts (median 6393.5 vs 328.5, $P = .041$) vs untreated FFPE. At 0.2 MAF threshold with UDG treatment, median TMB was 5.48 (range 1.68-16.07) and did not correlate with salient pathologic features of HCC, including survival.

Conclusion: While tNGS on fresh HCC samples appears to be the optimal source of tumour DNA, the low median TMB values observed may limit the role of TMB as a predictor of response to immunotherapy in HCC.

KEYWORDS

hepatocellular carcinoma, immunotherapy, tumour mutational burden

Ching Ngar Wong and Petros Fessas contributed equally to manuscript.

Handling editor: Ana Lleo

1 | INTRODUCTION

Hepatocellular carcinoma (HCC) is a malignancy with rising global incidence and a poor prognosis.[1] Although treatment is curative in early stages, when surgical resection or transplantation can be employed, many patients are diagnosed at a late stage.[2] Inoperable HCC is amenable to transarterial chemoembolization (TACE) or systemic therapy with targeted kinase inhibitors, such as sorafenib and lenvatinib.[3] In recent years, immune checkpoint inhibition (ICI) has become an emerging option for systemic therapy in advanced HCC.[4]

In HCC, the high levels of expression of immune checkpoint proteins, such as programmed cell death protein (PD-1) and its ligands (PD-L1 and PD-L2), alongside the prominence of immune suppressive cells in the HCC microenvironment,[5] provide a biologic rationale for the use of immune checkpoint blockade-targeted immunotherapy, and led to its investigation in clinical trials. Monoclonal agents against the PD-1 pathway, such as nivolumab and pembrolizumab, have been approved as second-line agents in advanced HCC.[4,6,7] However, the response rate to immunotherapy is approximately 20%.[8] While immunotherapy combinations are disrupting treatment paradigms in advanced HCC by inducing higher response rates and more convincing evidence of survival benefit, response to immunotherapy remains limited to a fraction of patients. When this is taken alongside the risk of treatment-related adverse events,[7] some of which being potentially life-threatening, the acute need for predictive biomarkers of response becomes apparent.

Tumour mutational burden (TMB) is an emerging genomic biomarker of response to immunotherapy.[8] TMB is defined as the number of somatic non-synonymous mutations per mega-base of assayed genome and can be computed from tissue or circulating tumour DNA using whole-exome or targeted next-generation sequencing (tNGS). Non-synonymous mutations can result in structurally distinct mutant protein products, which can act as neoantigens, increasing the probability of T-cell recognition of the tumour.[9] As a result, a higher number of non-synonymous mutations may account for clinically meaningful increase in the probability of response to immunotherapy, lending TMB as a putative genomic trait that can be used to stratify patients on the basis of their likelihood of response to ICI.[10-15]

In the field of HCC, a conclusive evaluation of the correlation between TMB and outcomes from immunotherapy is not available to date, largely because of the low proportion of patients requiring histological confirmation of the diagnosis prior to treatment.[16] Furthermore, most studies evaluating TMB as a predictive biomarker have utilized whole-exome sequencing techniques, which are expensive, characterized by long turnaround times and require bioinformatic expertise for interpretation.[17] For TMB to be a valuable and clinically applicable response biomarker in HCC, it requires a method of derivation from routinely collected samples that is reproducible and feasible in day-to-day clinical practice. In this pilot study, we describe the optimization of TMB estimation using tNGS on archival and fresh HCC samples in a view to facilitate its development as a biomarker of response to ICI.

Lay Summary

Number of mutations in tumour tissue (TMB) predict for outcome from immunotherapy. Here, we describe the challenges in optimizing TMB as a biomarker in hepatocellular cancer. Targeted next-generation sequencing on freshly collected tissue yields best results in TMB quantification.

2 | MATERIALS AND METHODS

2.1 | Patient cohort

Samples from 60 HCC patients were included in the study. Samples were derived from the Imperial College Healthcare NHS Trust tissue bank and included biopsies or resections performed between 2000 and 2019. All subjects gave their informed consent for inclusion in research prior to sample retrieval.

A subset of our patients (n = 4) was treated with pembrolizumab 200 mg intravenously every 3 weeks until subject withdrawal due to disease progression or toxicity. In these patients, tumours were biopsied at 28 days prior to dosing.

2.2 | Sample preparation

Samples were provided either as formalin-fixed paraffin-embedded (FFPE) blocks or fresh-frozen (FF) tissues.

FFPE tissue blocks were sectioned into 5 μm slices using a microtome and macro-dissected to ensure >20% tumour content. EchoSAFE FFPE Deparaffinization Solution kit (BioEcho Life Science GmBH, Germany) was used to deparaffinize sectioned FFPE tissue slices, using four slices of 5 μm FFPE tissue sections for each sample. The type, amount and working conditions of lysis buffer and proteinase followed instruction of AllPrep® DNA/RNA FFPE kit (QIAGEN, Venlo, NL, USA). Fresh-frozen tissues were placed on dry ice and sectioned into cubes of <30 mg using a sterilized scalpel.

2.3 | Nucleic acid extraction and preparation

In total, 60 tumour tissue samples (39 FFPE and 21 FF) were utilized. From FFPE tissues, DNA was extracted using AllPrep® DNA/RNA FFPE kit (QIAGEN). Lysis buffer loading and proteinase were performed during the deparaffinization step, as per the EchoSAFE FFPE Deparaffinization protocol. Sectioned FF cubes were placed into 2.0 mL tubes containing 1.4 mm Precellys ceramic beads (Bertin Instruments, Montigny-le-Bretonneux, France) and homogenized by Precellys 24 homogenizer (Bertin Instruments). RNA, DNA and proteins were extracted using AllPrep® DNA/RNA/Protein Mini kit (QIAGEN). To minimize the effect of cytosine deamination-induced mutation artefacts on TMB, FFPE samples were treated with

heat-liable uracil-DNA glycosylase (UDG) (Thermo Fisher Scientific, Loughborough, UK), according to the Oncomine™ TML assay protocol. Absorbance-based NanoDropTM 1000 Spectrophotometer (Thermal Fisher Scientific) was used for both DNA and RNA quantification. Fluorescence-based Qubit® double-stranded DNA High Sensitivity Assay Kit (Life Technologies, Carlsbad, Germany) was performed for further DNA quantification.A

Formalin-fixed paraffin-embedded tissue DNA samples with $A_{260/280}$ above 1.7 and $A_{260/230}$ above 1.7 measured by NanoDrop™ spectrophotometer were prioritized, and those with adequate intact double-strand DNA quantity (≥3.08 ng/μL) measured by Qubit® 2.0 fluorometer (Life Technologies) were selected for UDG treatment and subsequent sequencing to obtain TMB and variant calls.

Fresh-frozen tissue DNA samples with $A_{260/280}$ above 1.7 and $A_{260/230}$ above 1.7 measured by NanoDrop™ spectrophotometer were prioritized, and those with adequate intact double-strand DNA quantity (≥0.67 ng/μL) were selected for the Oncomine™ TML assay library preparation.

2.4 | Gene-targeted panel sequencing

The Ion Torrent™ Oncomine™ Tumour Mutation Load (TML) Assay was employed for tissue DNA sequencing. Ion AmpliSeq™ library preparation kit (Life Technologies) was employed for use with Chef DL8 (Life Technologies) on the automated Ion Chef™ system (Life Technologies).

Diluted UDG-treated FFPE DNA samples or FF DNA samples were loaded into the Ion Torrent™ 96-well PCR plate containing sample-specific barcodes and proceeded for library preparation.

Gene-specific primer pools of Ion Torrent™ Oncomine™ TML Assay (Life Technologies) were employed, targeting 408 genes for tumour profiling (Table S1).

The Torrent Suite online platform (Thermo Fisher Scientific) was used to input and record sample details for library preparation and templating. RNase-free water-diluted libraries at 50 pmol/L in 25 μL were loaded into Ion Chef™ system for templating onto the Ion 540™ Chips (Life Technologies).[18] Freshly templated chips were placed into Ion S5™ sequencer (Life Technologies) for tNGS within 1 hour of completion of templating.

Samples with uniformity and mean depth coverage over 80% and 300, respectively, in the quality control report of the sequence run were selected for further data analyses. Among 48 sequenced tissue samples, a final pool of 30 tissue samples (six untreated FFPE; six UDG-treated FFPE; and 18 FF) from 29 patients passed sequencing quality check and were subjected to downstream analyses.

2.5 | Data analysis

The Ion Reporter (Thermo Fisher Scientific) online platform and 'Oncomine TML -w2.0-DNA-Single Sample' analysis workflow were employed to calculate the TMB of samples. Minimum allele frequency (MAF) thresholds were adjusted to 10% and 20% as compared to default 5% for optimization.

Data were stratified according to sample preservation methods (FFPE vs FF), DNA pretreatment groups (untreated FFPE vs UDG-treated FFPE), MAF filtering thresholds in analysis workflow (MAF0.05 vs MAF0.1 vs MAF0.2), immunotherapy responses (responder vs non-responder), clinical parameter statuses (presence vs absence) and TMB groups (high vs low cut-off by median). Clinicopathologic data including patient demographics, tumour size and stage, liver function, plasma alpha foetoprotein (AFP) level, status of hepatitis viral infection, pattern of alcohol intake and survival were analysed anonymously for their relationship with TMB.

All statistical tests were performed with IBM SPSS Statistics (IBM Corporation, Armonk, NY, USA) software package. Mann-Whitney and Kruskal-Wallis tests were performed in two-tailed non-parametric manner to illustrate statistical differences of TMB in different parameter groups. Kaplan-Meier survival plots were constructed and log-rank (Mantel-Cox) tests were performed to examine the effect of TMB level on patient's overall survival (OS). We performed non-parametric Spearman Rho's test to investigate the association between TMB level and tumour size.

3 | RESULTS

3.1 | Patient cohort

In total, 48 archival tissues samples from 47 patients who underwent liver resection (n = 16), TACE (n = 9) or transplantation (n = 6) for HCC were included (FFPE n = 27; FF n = 21) (Figure 1). Samples were sequenced using the Oncomine™ TML Assay. The final analysis included 30 samples from 29 patients following exclusion of 18 samples that did not meet quality criteria for analysis (ie uniformity >80% and mean depth coverage >300). Clinical features of 29 evaluable patients are described in Table 1. The majority of patients included were male (83.9%) and cirrhotic (83.9%).

3.2 | Optimization of TMB measurement

A total of 30 tissue DNA samples from 29 patients that were sequenced utilizing the Oncomine™ TML assay panel satisfied the quality criteria for uniformity and coverage of sequencing and were deemed suitable for downstream analysis. We optimized the TMB measurement by comparing total number of non-synonymous mutations, deamination counts, somatic variant counts and non-synonymous variant counts and somatic mutation signatures according to different sample preservation methods (FFPE vs FF sample), DNA pretreatment methods and MAF thresholds in post-sequencing analysis.

We noted that FFPE DNA displayed significantly higher TMB (median 958.39 vs 2.51 Mut/Mb, IQR 9901.79 vs 3.77, $P < .0001$), estimated deamination counts (median 1335.50 vs 0, IQR 16 075 vs 1,

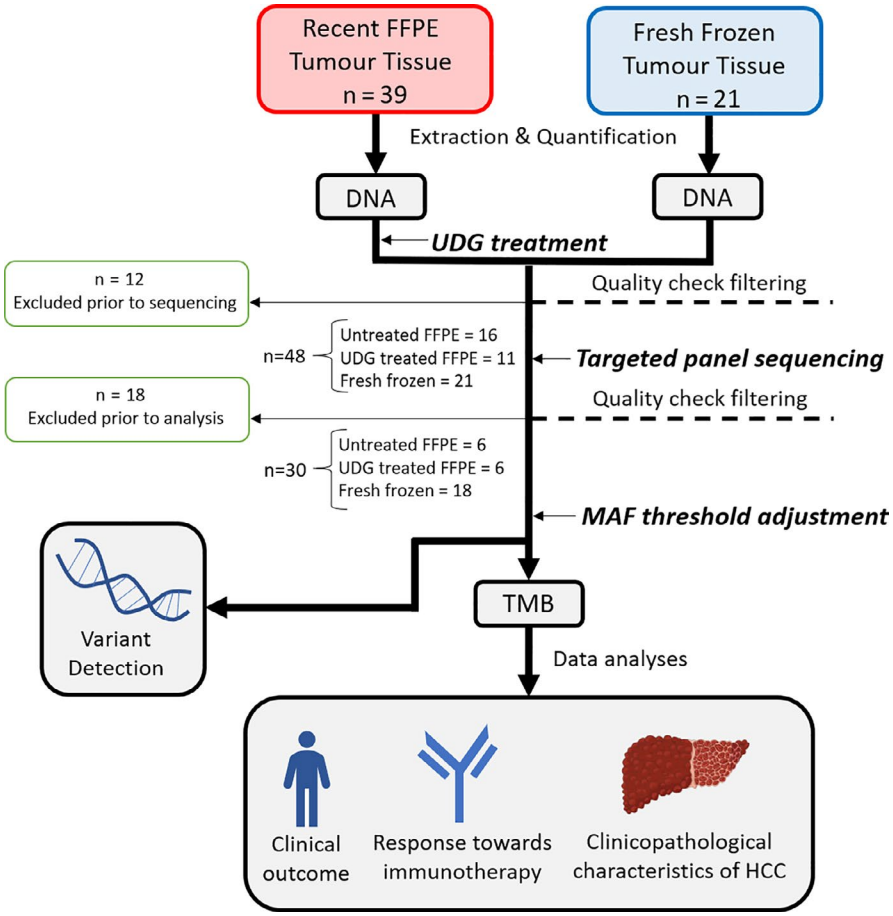

FIGURE 1 Schematic diagram to show sample disposition and processing. After extraction and quantification, DNA derived from FFPE tumour tissue was treated with UDG. Following this, samples that passed quality check and underwent targeted panel sequencing using Oncomine™TML assay. After further quality check filtering and selection and MAF threshold adjustment, TMB measurement and variant calling were performed. TMB was then correlated with patient data on clinical parameters and outcomes. FFPE, formalin-fixed paraffin-embedded; HCC, hepatocellular carcinoma; MAF, minimum allele frequency; TMB, tumour mutational burden; TML, Tumour Mutation Load; UDG, uracil-DNA glycosylase

$P < .0001$), somatic variant counts (median 1622.5 vs 6, IQR 17 240 vs 8, $P < .0001$) and non-synonymous variant counts (median 786.5 vs 3, IQR 4185 vs 4.5, $P < .0001$), when compared to FF tumour samples (Figure 2). Over three quarters of FFPE samples had TMB and deamination counts exceeding the maximum acceptable thresholds (ie TMB ≤ 100 Mut/Mb; deamination count ≤30), while all FF samples yielded interpretable TMB values and acceptable deamination counts.

Uracil-DNA glycosylase treatment was performed prior to sequencing of FFPE samples to optimize TMB measurement. UDG-treated FFPE samples carried significantly lower TMB (median 4019.92 vs 353 Mut/Mb, IQR 7730.91 vs 400.83, $P = .041$), estimated deamination counts (median 6393.5 vs 328.5, IQR 12 085.75 vs 310, $P = .041$), somatic variant counts (median 6901.5 vs 548, IQR 17 179 vs 578, $P = .041$) and non-synonymous variant counts (median 3227 vs 294, IQR 7980 vs 323, $P = .041$; Figure 3).

Formalin-fixed paraffin-embedded samples displayed significantly higher proportion of C > T transitions at CpG sites, including at AG[CG] and at CT[CG], and especially C > T transition at NCC, CC[ACT] and TC[ACT] (median 60.3% vs 9.1%, $P = .002$) (Table S1). UDG-treated FFPE had significantly lower C > T transitions at non-CpG sites, including NCC, CC[ACT] and CT[ACT] ($P = .041$), and C > T at other sites ($P = .041$), for an overall reduction of over 96%. Although this did not reach statistical significance, at CpG sites there was a reduction of over 50%, including [AG]CG ($P = .180$) and [CT]CG ($P = .240$) (Table S2).

At the default MAF for detection of 5%, UDG-treated FFPE and untreated FFPE had cumulatively over 90% of somatic variant allele frequency clustered and skewed at class intervals below 20% allele frequency. FF samples displayed more normally distributed allele frequencies, peaked between 40%-50% and 50%-60% class interval allele frequencies, and less than 20% of somatic variants detected were clustered at allele frequency class intervals below 20%, that is 5%-10% and 10%-20% (Figure 4).

In UDG-treated (UDG+) and untreated (UDG−) FFPE samples, adjustment from MAF0.05 to MAF0.2 resulted in significantly reduced TMB ($P = .002$ for UDG+, $P = .009$ for UDG−), estimated deamination counts ($P = .001$ for UDG+ and UDG−), somatic variant counts ($P = .002$ for UDG+, $P = .009$ for UDG−) and non-synonymous variant counts ($P = .001$ for UDG+, $P = .009$ for UDG−) (Figures S1 and S2). There was a significant reduction in all somatic mutation signatures (ie C > T at [AG]CG, [CT]CG, NCC/CC[ACT]/TC[ACT] sites or others) (Table S3). Overall, raising MAF threshold to 20% resulted in both interpretable TMB and acceptable deamination counts.

In FF samples, comparison of MAF thresholds applied revealed no statistically significant differences in TMB ($P = .833$), estimated deamination counts ($P = .254$), somatic variant counts ($P = .840$) and non-synonymous variant counts ($P = .850$) among all three MAF thresholds (Figure S3). All TMB and deamination counts derived from all three MAF thresholds were interpretable and acceptable.

TABLE 1 Clinical characteristics of patient samples passing sequencing quality check (ie uniformity > 80% and mean depth coverage > 300)

Characteristics	n = 29, (%)
Gender	
Male	24 (83)
Female	5 (17)
Age, median (range)	62 (34 to 89)
Cirrhosis	24 (83)
HBV infection	3 (10)
HCV infection	13 (45)
Alcoholic consumption	13 (45)
Alpha foetoprotein level, median (range)	55.5 (0 to 74,584)
<400	17 (59)
>400	5 (17)
Unknown	7 (24)
Treatment, n = 29	
Resection	16 (55)
Transarterial chemoembolization	9 (31)
Transplantation	6 (21)
Pembrolizumab	4 (14)
Immunotherapy response, n = 4	
Responder	2
Non-responder	1
Unclassified	1

Moreover, there were no statistically significant differences in any somatic mutation signature counts ($P > .8$) by MAF threshold adjustment (Table S4).

Comparison of untreated FFPE to FF samples at MAF0.2 threshold revealed significantly higher TMB (median 34.79 vs 1.69 Mut/Mb, IQR 93.99 vs 2.94, $P = .017$), somatic variant counts (median 90 vs 5, IQR 201.5 vs 6, $P = .003$) and non-synonymous variant counts (media 37 vs 2, IQR 83.75 vs 4, $P = .010$) in untreated FFPE samples. By contrast, comparison of UDG-treated FFPE to FF samples did not show any statistical differences in TMB (median 5.48 vs 1.69 Mut/Mb, IQR 8.11 vs 2.94, $P = .291$), somatic variant counts (median 15 vs 5, IQR 17 vs 6, $P = .069$) and non-synonymous variant counts (median 6 vs 2, IQR 10 vs 4, $P = .238$). This demonstrated that MAF adjustment alone was not sufficient to optimize TMB measurement, while combination of UDG treatment and MAF threshold adjustment to 20% led to a reduction in TMB values to best match the levels measured in FF samples (Figure 5).

Finally, we evaluated the impact of MAF threshold readjustment in variant calling in FFPE and FF samples. At MAF0.2, there were 112 non-synonymously mutated genes found in untreated FFPE samples, 38 found in UDG-treated FFPE samples and 32 found in FF samples. Collectively, 34 non-synonymously mutated genes and gene combinations were found in two or more sample groups at MAF0.2 threshold, and only two genes (ie *KMT2C* and *TAF1L*) were found common among all sample groups (Table 2).

3.3 | Relationship between TMB and clinical outcomes

In our cohort, median OS was 12.3 months (95% CI 1-40). OS was stratified based on median TMB detected at MAF0.2 threshold in untreated FFPE, UDG-treated FFPE and FF samples independently (Figure 6). Comparison of OS in low vs high MAF0.2 TMB groups of untreated FFPE ($P = .114$), UDG-treated FFPE ($P = .988$) and FF ($P = .738$) samples was not statistically significan

Correlation of TMB to clinical-pathological outcomes of patients was tested independently for untreated FFPE, UDG-treated FFPE and FF samples due to differential distribution of TMB at MAF0.2 threshold among sample groups. Tumour size was significantly correlated with TMB at MAF0.2 threshold in untreated FFPE samples (correlation coefficient = .88, $P = .021$), while no statistical correlation to TMB at MAF0.2 threshold was observed in UDG-treated FFPE (correlation = .205, $P = .741$) and FF (correlation = .375, $P = .153$) (Figure S4). There was no significant correlation between TMB and viral infection status, presence of cirrhosis, alcohol consumption and level of plasma AFP, across all sample groups ($P > .05$ for all correlations).

Of the 34 genes found to be non-synonymously mutated across two sample groups, four genes were highlighted as commonly found in top 20 mutated genes in HCC reported in COSMIC database and in our study at MAF0.2 threshold. OS of patients was stratified according to the mutation status of genes. Among these four genes, that is *KMT2D* ($P = .771$), *KMT2C* ($P < .001$), *HNF1A* ($P = .652$) and *LRP1B* ($P = .586$), mutation of *KMT2C* demonstrated significantly shorter OS duration in patients (30.1 vs 1 month).

Our cohort included four patients with sequenced FF DNA treated with pembrolizumab. Their OS from diagnosis ranged from 0.9 to 13.1 month(s). Only three patients were evaluable for response based on RECIST 1.1 criteria and were included in our exploratory analysis. Response was observed in two of three patients. Comparison of TMB at MAF0.2 between patients who achieved an objective response and those who did not revealed no statistical differences (median 0.745 vs 0 Mut/Mb, $P = 1.000$). Three non-synonymously mutated genes, *CIC*, *PIK3R1* and *TSC2*, were detected at default MAF 5% threshold in immunotherapy recipients. All patients carried missense mutations in *CIC* gene and one responder carried missense mutation for all three genes.

4 | DISCUSSION

The treatment landscape of advanced HCC is changing at a rapid pace, with ICI having become a therapeutic option as a first- and second-line therapy in patients with unresectable disease.[19] The choice between immunotherapy combination between atezolizumab and bevacizumab in first-line, over PD-1 targeting agents [20,21] with or without CTLA-4 inhibitors in second-line,[22] is dictated by clinical characteristics of the patients and reimbursement considerations. There are no reliable biomarkers to allow effective molecular triaging

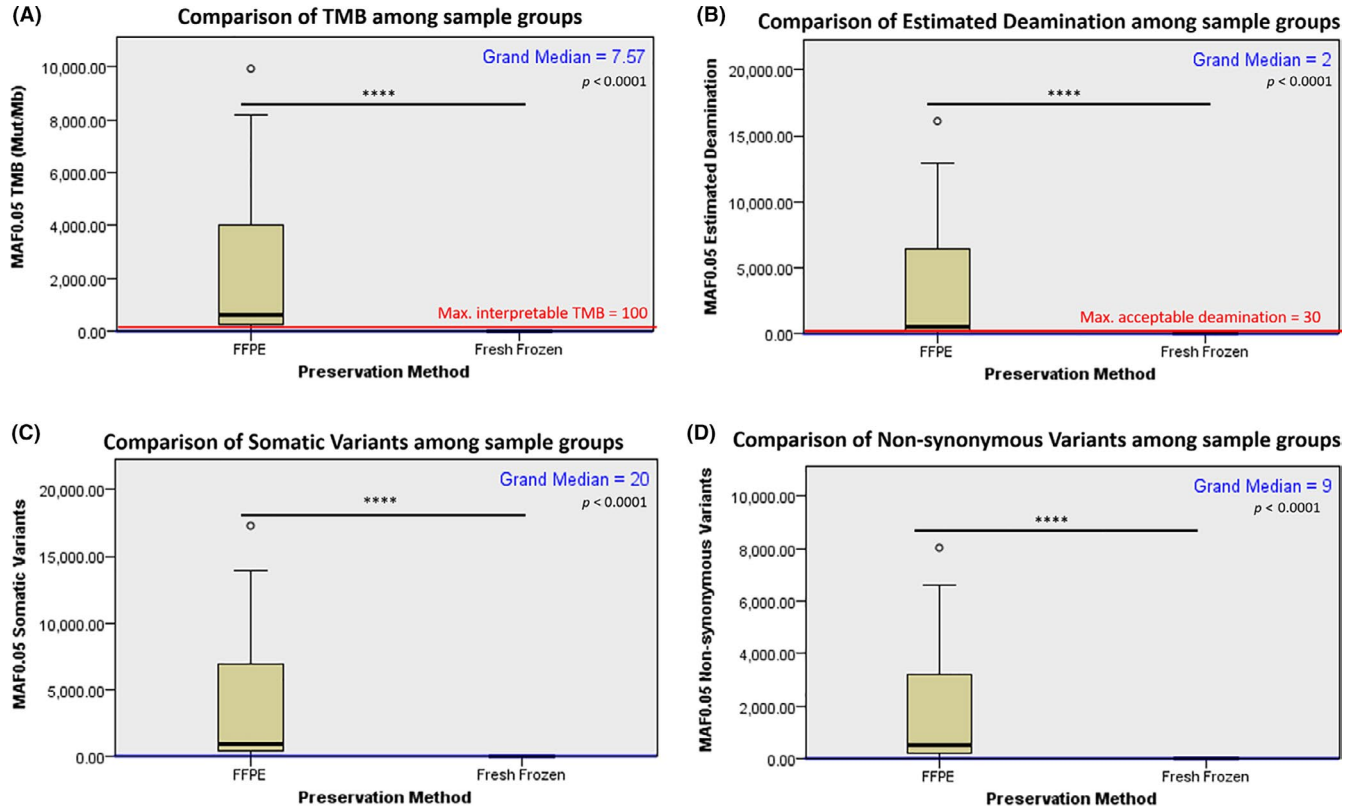

FIGURE 2 Box-and-Whisker plots to show comparison of (A) TMB, (B) estimated deamination, (C) somatic variants and (D) non-synonymous variants between sample preservation method groups (FFPE vs fresh-frozen tumour tissue) at default filter chain setting (MAF0.05) by non-parametric two-tailed Mann-Whitney*U*test. Total n = 25 (FFPE = 12; fresh-frozen = 13). Maximum interpretable TMB = 100 Mut/Mb; maximum acceptable estimated deamination count = 30. Level of statistical significance indicated by *<.05; **<.01; ***<.001 and ****<.0001. FFPE, formalin-fixed paraffin-embedded; MAF, minimum allele frequency; TMB, tumour mutational burden

of patients towards the most appropriate therapy in HCC, where PD-L1 immunostaining has demonstrated limited reproducibility and inadequate linkage with clinical outcomes.[23-25] Genomic determinants of response to immunotherapy have been under intense scrutiny across malignancies. For instance, the presence of mutations in the beta-catenin pathway has been associated with an immune-excluded phenotype in HCC,[26] suggesting a therapeutically appealing relationship between mutations in candidate loci and the immune suppressive characteristics of the tumour microenvironment.

Tumour mutational burden is an emerging biomarker of response to immunotherapy across oncological indication. Tumours harbouring higher levels of non-synonymous mutations by whole-exome sequencing analysis have been shown to be intrinsically responsive to immunotherapy.[27]

In this pilot study, we aimed to verify whether tNGS can be routinely utilized as a measure of patients' TMB in patients with HCC. Unlike WES, tNGS is widely available across institutions, being routinely employed for testing of actionable mutations in solid tumours. tNGS platforms with lower coverage and depth of sequencing have been successfully implemented as a way of testing for patients' TMB status in tumours other than HCC.[28] Moreover, tNGS is generally suitable for analysis of FFPE samples.[29]

Using a commercially available TMB platform, we optimized the methodology of TMB measurement in archival and fresh samples from patients with HCC and evaluated TMB as a prognostic biomarker for this condition.

During optimization, we reproduced the finding that FFPE samples contain more deaminated artefact mutations than FF samples.[30,31] Specifically, we found significantly higher C > T deamination at [AG]CG and [CT]CG, which were at CpG sites; as well as C > T deamination at NCC, CC[ACT] and TC[ACT], compared to FF samples. In absence of any treatment, the levels of TMB appeared to be significantly altered by fixation artefacts, making interpretation of patients' TMB status particularly challenging. These findings bring to question the practicality of using FFPE samples to derive TMB as a biomarker. To address this, we investigated the ways of reducing the amount of deamination artefact in FFPE sample with UDG treatment prior to sequencing. UDG is an enzyme that prevents mutagenesis by eliminating from DNA molecules the uracil that results from cytosine deamination. Although UDG treatment achieved a reduction of TMB and deamination by over 90%, TMB values remained above the recommended interpretable limit of 100 Mut/Mb, while deamination counts remained above 30/Mb.

In order to achieve interpretable TMB levels, we investigated the effect of adjusting the MAF threshold to filter low prevalent mutations that are likely to represent artefacts. Regardless of DNA pretreatment with UDG, the significantly lowered TMB and deamination base counts, and significant reduction in all mutation

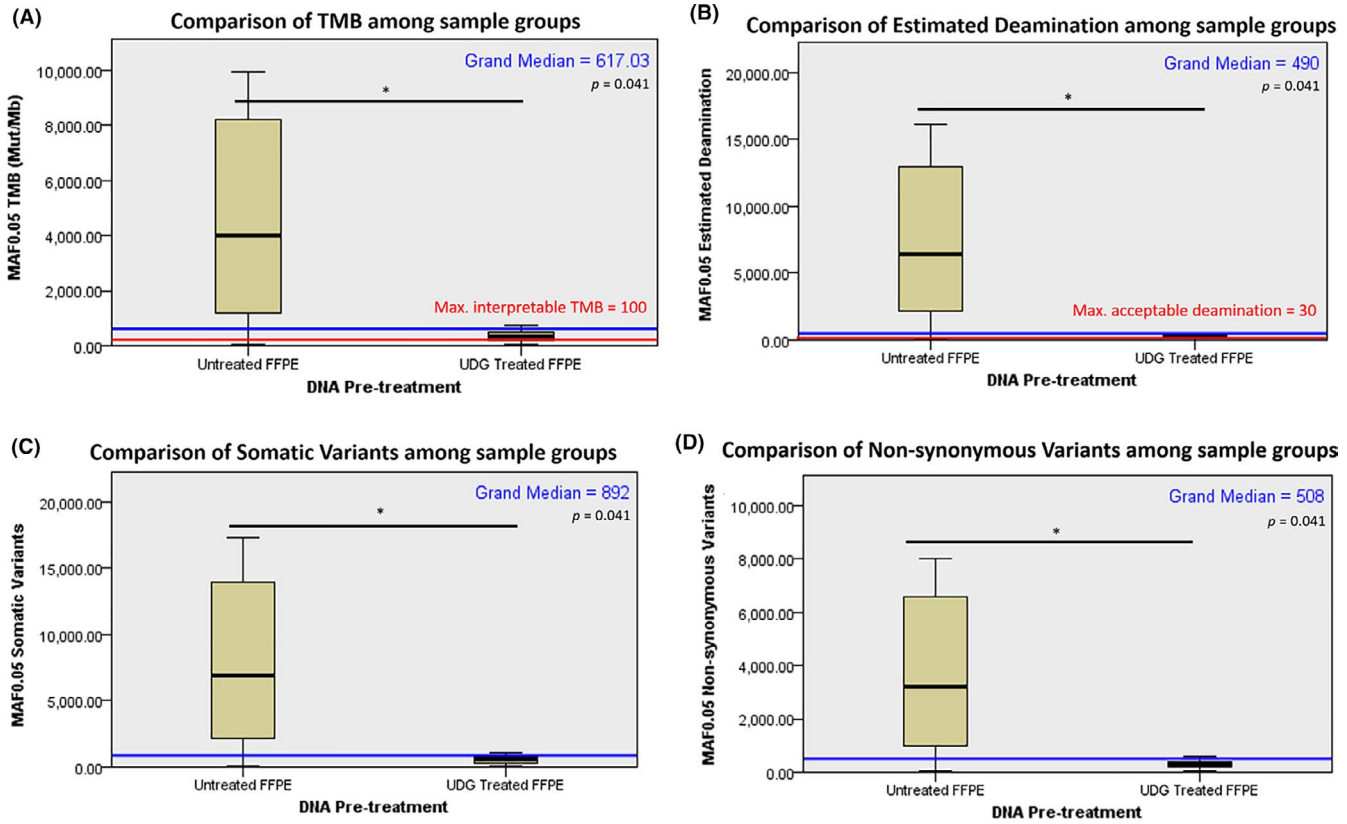

FIGURE 3 Box-and-Whisker plots to show comparison of (A) TMB, (B) estimated deamination, (C) somatic variants and (D) non-synonymous variants between DNA pretreatment groups (untreated FFPE vs UDG-treated FFPE) at default filter chain setting (MAF0.05) by non-parametric two-tailed Mann-Whitney*U*test. Total n = 12 (untreated FFPE = 6; UDG-treated FFPE = 6). Maximum interpretable TMB = 100 Mut/Mb; maximum acceptable estimated deamination count = 30. Level of statistical significance indicated by *<.05; **<.01; ***<.001 and ****<.0001. FFPE, formalin-fixed paraffin-embedded; MAF, minimum allele frequency; TMB, tumour mutational burden; UDG, uracil-DNA glycosylase

FIGURE 4 Percentage distribution of somatic variant allele frequency of UDG-treated FFPE, untreated FFPE and fresh-frozen tumour tissue samples. Total n = 25 (UDG-treated FFPE = 6; untreated FFPE = 6; fresh-frozen = 13), 408 genes included for allele frequency detection at default MAF0.05 filtering threshold. Error bar presented in one standard error from mean value. FFPE, formalin-fixed paraffin-embedded; MAF, minimum allele frequency; UDG, uracil-DNA glycosylase

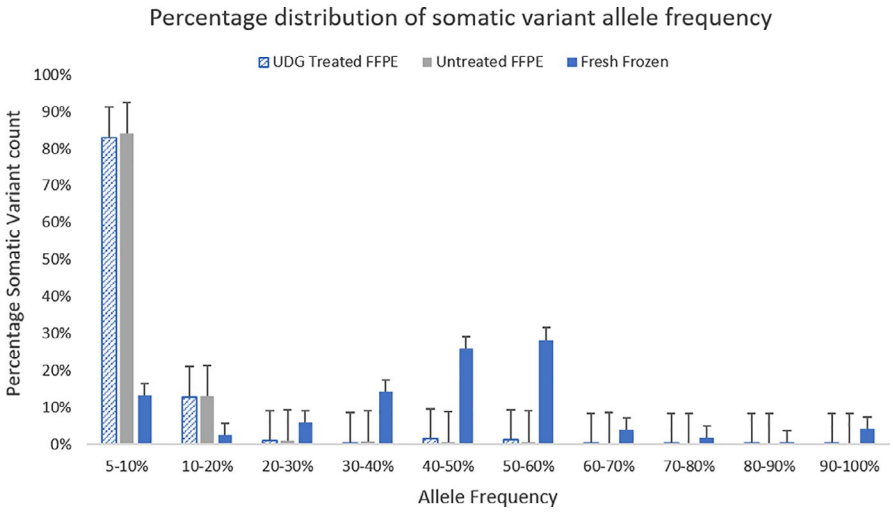

signature patterns under MAF0.2 threshold over MAF0.05 revealed that adjustment of MAF threshold to 20% was effective in reducing the impact of fixation artefacts in affecting the overall TMB reading. MAF threshold adjustment proved an effective methodology for all sample groups, with most FFPE and all FF samples attaining interpretable TMB level under MAF0.2 threshold. Additionally, adjustment to MAF0.2 greatly reduced the differences in the number of mutations detected between FFPE and FF samples (Figures 2 and 4), highlighting its importance for variant detection alongside TMB measurement. Altering the MAF threshold increased the probability

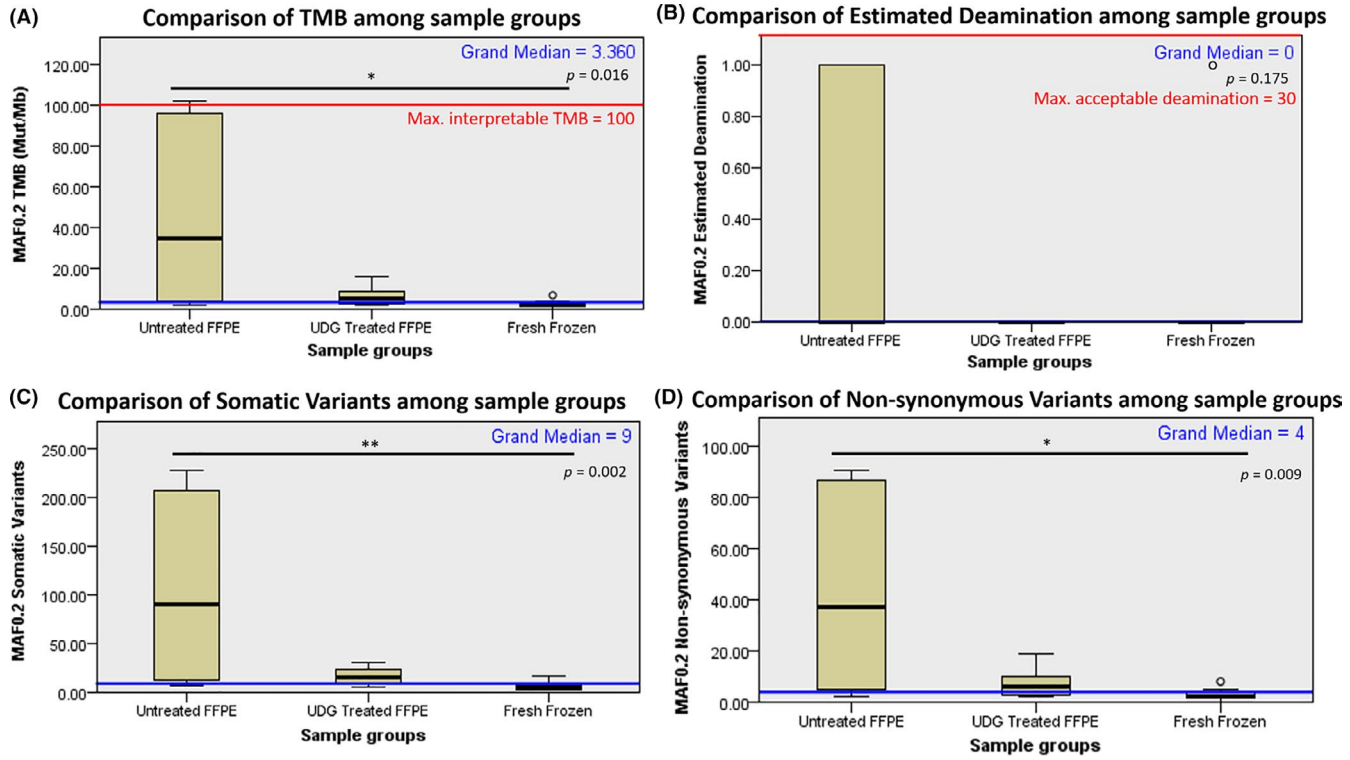

FIGURE 5 Box-and-Whisker plots to show comparison of (A) TMB, (B) estimated deamination, (C) somatic variants and (D) non-synonymous variants between sample groups (untreated FFPE vs UDG-treated FFPE vs fresh-frozen) at Oncomine™ Tumour Mutation Load (TML) assay filter chain MAF0.2 threshold by non-parametric two-tailed Kruskal-Wallis test with multiple comparisons. Total n = 25 (untreated FFPE = 6; UDG-treated FFPE = 6; fresh-frozen = 13). Maximum interpretable TMB = 100 Mut/Mb; maximum acceptable estimated deamination count = 30. Level of statistical significance indicated by *<.05; **<.01; ***<.001 and ****<.0001. FFPE, formalin-fixed paraffin-embedded; MAF, minimum allele frequency; TMB, tumour mutational burden; UDG, uracil-DNA glycosylase

of filtering out low-frequency variables that are subclonal in nature and reflect intratumour heterogeneity (ITH), something which has been reported previously in HCC at a frequency of 5%-10%.[32] Indeed, in our FF samples, approximately 10% of variants were detected at 5%-10% allele frequency and may be accounted for by ITH. It follows, therefore, that MAF threshold adjustment to 0.2 in FFPE samples may render ITH indistinguishable from mutation artefact but permits more accurate TMB calculations.

Comparison of TMB under MAF0.2 derived from UDG-treated FFPE to that derived from untreated FFPE samples demonstrated that UDG treatment further reduced the TMB value and deamination artefact contributions from FFPE-related sites (ie C > T at NCC, CC[ACT] and TC[ACT]). The combined effects of UDG treatment and MAF adjustment were shown significant by comparison of TMB under MAF0.05 threshold from untreated FFPE to TMB under MAF0.2 threshold from UDG-treated FFPE. Therefore, combined UDG treatment with MAF0.2 threshold adjustment is expected to lend to best outcomes on both TMB interpretation as well as single variant detection.

Following optimization, the correlation of TMB with common clinicopathological outcomes and features was investigated. We concentrated on a subset of samples that were adequate based on stringent quality control criteria (Figure 1). Due to the fact that TMB values were found to distribute differently across preservation and presequencing treatment sample groups, samples were stratified according to how they were prepared, due to the limited availability of matched untreated FFPE, UDG-treated FFPE and FF samples from the same individual.

Tumour size was the only feature found to correlate with TMB, and this was found in untreated FFPE samples. This is in keeping with a previous study in HCC, which did not demonstrate a correlation between TMB or other genomic differences and clinical outcomes, including OS.[16] However, it should be noted that the fairly limited sample size and stage heterogeneity of our cohort preclude us from drawing definitive conclusions as to the prognostic role of TMB in HCC, a point that should be explored in future studies.

Among the non-synonymously mutated genes derived from targeted sequencing, we looked at specific mutations known to be more prevalent in HCC and investigated their impact on outcome. The gene *KMT2C* was detected at both MAF0.05 and MAF0.2 thresholds among all sample groups and was found to be significantly associated with OS. Detection of *KMT2C*, one of the top 20 cancer-driving mutations for HCC in the COSMIC database, confirms that potential key driver mutations in HCC are detectable in a panel selected for tNGS in our study.

Our investigation of the use of TMB as a prognostic biomarker for immunotherapy in HCC was limited by the small number of patients,

TABLE 2 Ranked list of non-synonymously mutated gene and gene combinations found in two or more sample groups (ie UDG-treated FFPE, untreated FFPE and fresh-frozen) based on mutation frequency. A total of 34 non-synonymously mutated genes and gene combinations were ranked based on mutation frequency. Asterisks (*) indicate genes appeared on the list of Top 20 mutated genes in HCC patients in the COSMIC database. Allele frequency of mutated genes detected at default 5% minimum allele frequency threshold. Mutation frequency was calculated by number of mutated samples per gene divided by number of total samples included. Total n = 30

Rank	Non-synonymously mutated gene/ gene combination at MAF0.2	Allele frequency range (%)		Mutation frequency (%)
		Lowest	Highest	
1	*KMT2D**	22.55	41.59	13.3
2	*TAF1L*	20.09	45.59	13.3
3	*ADGRA2*	20.00	23.76	10.0
4	*ADGRL3*	28.57	59.07	10.0
5	*BCYRN1|TAF1*	22.76	33.73	10.0
6	*CREBBP*	24.76	51.43	10.0
7	*EP300*	23.23	47.99	10.0
8	*GATA1*	20.00	22.15	10.0
9	*KDM5C*	20.36	30.53	10.0
10	*KMT2C**	22.70	33.25	10.0
11	*NOTCH4*	21.05	26.69	10.0
12	*NTRK1*	24.81	36.79	10.0
13	*TBX22*	21.55	56.74	10.0
14	*ACVR2A*	22.86	87.00	6.7
15	*AFF3*	21.74	39.96	6.7
16	*AKAP9*	29.33	44.62	6.7
17	*ASXL1*	20.61	42.68	6.7
18	*BLM*	20.88	51.10	6.7
19	*CDKN2B*	22.86	24.71	6.7
20	*CSF1R*	22.14	66.67	6.7
21	*CSMD3*	27.21	40.54	6.7
22	*HNF1A**	22.92	39.11	6.7
23	*ITGB3*	47.57	48.59	6.7
24	*LRP1B**	21.80	29.07	6.7
25	*MAGEA1*	20.41	99.81	6.7
26	*MAML2*	26.47	53.38	6.7
27	*MN1*	21.88	22.43	6.7
28	*NBPF19*	22.77	39.53	6.7
29	*NBPF20*	22.00	23.21	6.7
30	*NF2*	20.18	32.32	6.7
31	*NUMA1*	20.29	50.83	6.7
32	*PAX3*	20.60	67.97	6.7
33	*RNF213*	22.29	31.07	6.7
34	*MAP2K2*	25.74	32.22	6.7

Note: Abbreviations: FFPE, formalin-fixed paraffin-embedded; HCC, hepatocellular carcinoma; UDG, uracil-DNA glycosylase.

with only three patients being evaluable following pembrolizumab treatment. As such, this study was not powered to detect the differences in TMB between immunotherapy responders and non-responders using the Oncomine™ TML assay, and can only provide a preliminary, descriptive evaluation. We found no difference in TMB distribution between responders and non-responders to immunotherapy, where no patients had TMB values >10 Mut/Mb. Further research is required to fully address this question.

We recognize significant limitations to our study. Firstly, we have to take into account inter-sample differences given the groups of untreated, UDG-treated FFPE and FF DNA samples were not extracted from the same tumours. In addition, DNA integrity is inversely proportional to the duration of tissue fixation.[33] Because our study included archival material processed during routine care, we cannot confidently reconstruct the influence of fixation on DNA quality. A better study design would have entailed pairwise

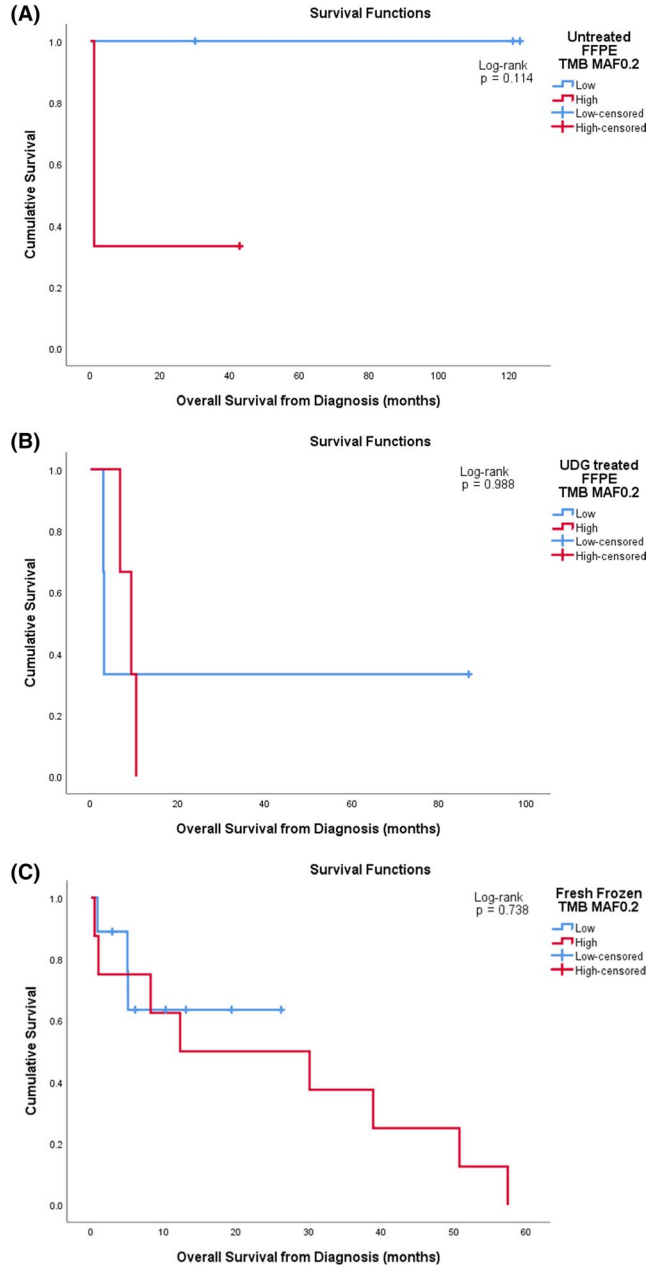

FIGURE 6 Overall survival (OS) of patients stratified according to TMB (low vs high based on median) at MAF0.2 threshold, calculated by Kaplan-Meier survival plot with log-rank (Mantel-Cox) test. Untreated FFPE samples shown in (A) OS (median 121.1 vs 1.03 mo,$P = .114$, n = 6); UDG-treated FFPE samples shown in (B) OS (median 3.1 vs 9.3 mo,$P = .988$, n = 6); and fresh-frozen samples shown in (C) OS (median 5.6 vs 12.3 mo,$P = .738$, n = 17). FFPE, formalin-fixed paraffin-embedded; MAF, minimum allele frequency; TMB, tumour mutational burden; UDG, uracil-DNA glycosylase

evaluation of fresh and FFPE samples from the same tumours, controlling for fixation time. Our study followed a more pragmatic design: to ensure sufficient statistical power to allow correlation with clinical outcomes, we opted to include the maximum number of consecutive patients to generate an adequate sample size for hypothesis testing. Another important limitation of this work is that there is lack of consensus in TMB cut-off threshold for HCC in the literature. Therefore, this study employed the median value of non-synonymous mutations as the cut-off threshold to stratify patients into 'high' and 'low' TMB groups. Lastly, our study did not address the impact of intratumoural heterogeneity on TMB estimation, a point of greater consequence given that regional expression of passenger mutations leads to clonal expansion of adaptive immune cells in HCC.[34]

5 | CONCLUSIONS

This study describes the optimization approaches for the determination of TMB in HCC at pre- and post-sequencing levels. Utilization of FF samples should be prioritized to avoid any fixation procedures. UDG treatment should be performed prior to sequencing of FFPE samples to minimize deamination artefacts in unmethylated CpG sites and non-CpG sites. MAF threshold adjustment to 20% in analysis filter chain should be applied to remove maximum number of deamination artefacts, while retaining optimal number of genuine mutations for TMB measurement as well as variant detection.

Overall, our pilot study has successfully optimized the Oncomine™ TML assay for measurement of TMB in HCC patients using FFPE and FF samples and highlights the challenges of reconstructing TMB using untreated, archival material. In this context, we outline our suggested methodology to optimize TMB measurement, and recommend fresh tissue to provide the highest chance of reliable readings. Future research is needed to fully evaluate whether TMB is a suitable biomarker for immunotherapy response in HCC patients. However, our findings of low TMB in this cohort suggest that it might not be a suitable response biomarker for this emerging treatment modality.

ACKNOWLEDGEMENTS

The authors acknowledge the infrastructure support provided by Imperial Experimental Cancer Medicine Centre, Cancer Research UK Imperial Centre and the Imperial College Healthcare NHS Trust Tissue Bank.

CONFLICT OF INTEREST

DJP received lecture fees from ViiV Healthcare and Bayer Healthcare and travel expenses from BMS and Bayer Healthcare; consulting fees for Mina Therapeutics, EISAI, Roche and Astra Zeneca; received research funding (to institution) from MSD and BMS.

AUTHOR CONTRIBUTIONS

DJP: Study concept and design. CNW, KD, PF, FAM, TK, PT, CA and DJP: Acquisition of data. CNW, DJP and KD: Analysis and interpretation of data. All the authors: Critical revision of the manuscript for important intellectual content. CNW: Statistical analysis.

DJP: Funding acquisition. DJP, KD, PDP, JK, RDG and FAM: Study supervision.

ORCID

Pierluigi Toniutto https://orcid.org/0000-0002-2566-3041
David J. Pinato https://orcid.org/0000-0002-3529-0103

REFERENCES

1. Bray F, Ferlay J, Soerjomataram I, Siegel RL, Torre LA, Jemal A. Global cancer statistics 2018: GLOBOCAN estimates of incidence and mortality worldwide for 36 cancers in 185 countries. *CA Cancer J Clin*. 2018;68:394-424.
2. Tang A, Hallouch O, Chernyak V, Kamaya A, Sirlin CB. Epidemiology of hepatocellular carcinoma: target population for surveillance and diagnosis. *Abdom Radiol*. 2018;43:13-25.
3. Contratto M, Wu J. Targeted therapy or immunotherapy? Optimal treatment in hepatocellular carcinoma. *World J Gastrointest Oncol*. 2018;10:108-114.
4. Iñarrairaegui M, Melero I, Sangro B. Immunotherapy of hepatocellular carcinoma: Facts and hopes. *Clin Cancer Res*. 2018;24:1518-1524.
5. Buonaguro L, Mauriello A, Cavalluzzo B, Petrizzo A, Tagliamonte M. Immunotherapy in hepatocellular carcinoma. *Ann Hepatol*. 2019;18:291-297.
6. FDA. FDA grants accelerated approval to pembrolizumab for hepatocellular carcinoma. [Internet]. https://www.fda.gov/drugs/fda-grants-accelerated-approval-pembrolizumab-hepatocellular-carcinoma. Accessed June 13, 2020
7. Rimassa L. Drugs in development for hepatocellular carcinoma. *Gastroenterol Hepatol*. 2018;14:542-544.
8. Yarchoan M, Hopkins A, Jaffee EM. Tumor mutational burden and response rate to PD-1 inhibition. *N Engl J Med*. 2017;377:2500-2501.
9. Riley TP, Keller GLJ, Smith AR, et al. Structure based prediction of neoantigen immunogenicity. *Front Immunol*. 2019;10:2047.
10. Büttner R, Longshore JW, López-Ríos F, et al. Implementing TMB measurement in clinical practice: considerations on assay requirements. *ESMO Open*. 2019;4:e000442. https://doi.org/10.1136/esmoopen-2018-000442
11. Goodman AM, Kato S, Bazhenova L, et al. Tumor mutational burden as an independent predictor of response to immunotherapy in diverse cancers. *Mol Cancer Ther*. 2017;16:2598-2608.
12. Guibert N, Jones G, Beeler JF, et al. Targeted sequencing of plasma cell-free DNA to predict response to PD1 inhibitors in advanced non-small cell lung cancer. *Lung Cancer*. 2019;1:1-6.
13. Rizvi NA, Hellmann MD, Snyder A, et al. Mutational landscape determines sensitivity to PD-1 blockade in non-small cell lung cancer. *Science*. 2015;348:124-128.
14. Le DT, Uram JN, Wang H, et al. PD-1 blockade in tumors with mismatch-repair deficiency. *N Engl J Med*. 2015;372:2509-2520.
15. Cristescu R, Mogg R, Ayers M, et al. Pan-tumor genomic biomarkers for PD-1 checkpoint blockade-based immunotherapy. *Science*. 2018;362:eaar3593.
16. Ang C, Klempner SJ, Ali SM, et al. Prevalence of established and emerging biomarkers of immune checkpoint inhibitor response in advanced hepatocellular carcinoma. [Internet]. *Oncotarget*. 2019;10:4018-4025. https://pmc/articles/PMC6592287/?report=abstract. Accessed June 26, 2020
17. Schwarze K, Buchanan J, Taylor JC, Wordsworth S. Are whole-exome and whole-genome sequencing approaches cost-effective? A systematic review of the literature. [Internet]. *Genet Med*. 2018;20:1122-1130. https://pubmed.ncbi.nlm.nih.gov/29446766/. Accessed June 24, 2020
18. Thermo Fisher Scientific. Ion 540 kit – chef user guide (Pub. No. MAN0010851 Rev. D.0).
19. Pinato DJ, Guerra N, Fessas P, et al. Immune-based therapies for hepatocellular carcinoma. [Internet]. *Oncogene*. 2020:1-18. http://www.nature.com/articles/s41388-020-1249-9. Accessed March 15, 2020.
20. Finn RS, Ryoo B-Y, Merle P, et al. Results of KEYNOTE-240: phase 3 study of pembrolizumab (Pembro) vs best supportive care (BSC) for second line therapy in advanced hepatocellular carcinoma (HCC). *J Clin Oncol*. 2019;37:4004.
21. Finn RS, Ducreux M, Qin S, et al. IMbrave150: A randomized phase III study of 1L atezolizumab plus bevacizumab vs sorafenib in locally advanced or metastatic hepatocellular carcinoma. *J Clin Oncol*. 2018;36:TPS4141.
22. FDA. FDA grants accelerated approval to nivolumab and ipilimumab combination for hepatocellular carcinoma. [Internet]. https://www.fda.gov/drugs/resources-information-approved-drugs/fda-grants-accelerated-approval-nivolumab-and-ipilimumab-combination-hepatocellular-carcinoma. Accessed June 25, 2020
23. Pinato DJ, Mauri FA, Spina P, et al. Clinical implications of heterogeneity in PD-L1 immunohistochemical detection in hepatocellular carcinoma: the Blueprint-HCC study. [Internet]. *Br J Cancer*. 2019;120:1033-1036. https://pubmed.ncbi.nlm.nih.gov/31061454/. Accessed June 25, 2020
24. Zhu AX, Finn RS, Edeline J, et al. Pembrolizumab in patients with advanced hepatocellular carcinoma previously treated with sorafenib (KEYNOTE-224): a non-randomised, open-label phase 2 trial. *Lancet Oncol*. 2018;19:940-952.
25. El-Khoueiry AB, Sangro B, Yau T, et al. Nivolumab in patients with advanced hepatocellular carcinoma (CheckMate 040): an open-label, non-comparative, phase 1/2 dose escalation and expansion trial. *Lancet*. 2017;389:2492-2502.
26. Harding JJ, Nandakumar S, Armenia J, et al. Prospective genotyping of hepatocellular carcinoma: Clinical implications of next-generation sequencing for matching patients to targeted and immune therapies. [Internet]. *Clin Cancer Res*. 2019;25:2116-2126. https://clincancerres.aacrjournals.org/content/early/2018/10/27/1078-0432.CCR-18-2293. Accessed June 28, 2020
27. Goodman AM, Kato S, Bazhenova L, et al. Tumor mutational burden as an independent predictor of response to immunotherapy in diverse cancers. [Internet]. *Mol Cancer Ther*. 2017;16:2598-2608. https://pubmed.ncbi.nlm.nih.gov/28835386/. Accessed June 25, 2020
28. Buchhalter I, Rempel E, Endris V, et al. Size matters: dissecting key parameters for panel-based tumor mutational burden analysis. [Internet]. *Int J Cancer*. 2019;144:848-858. https://pubmed.ncbi.nlm.nih.gov/30238975/. Accessed June 25, 2020
29. Pinato DJ, Urus H, Newsom-Davis T, et al. Applicability of routine targeted next-generation sequencing to estimate tumor mutational burden (TMB) in patients treated with immune checkpoint inhibitor therapy. [Internet]. *J Immunother*. 2020;43:53-56. https://pubmed.ncbi.nlm.nih.gov/31567705/. Accessed June 25, 2020.
30. Spencer DH, Sehn JK, Abel HJ, Watson MA, Pfeifer JD, Duncavage EJ. Comparison of clinical targeted next-generation sequence data from formalin-fixed and fresh-frozen tissue specimens. *J Mol Diagn*. 2013;15:623-633.
31. Wong SQ, Li J, Tan AYC, et al. Sequence artefacts in a prospective series of formalin-fixed tumours tested for mutations in hotspot regions by massively parallel sequencing. *BMC Med Genomics*. 2014;7(1):23.
32. Friemel J, Rechsteiner M, Frick L, et al. Intratumor heterogeneity in hepatocellular carcinoma. *Clin Cancer Res*. 2015;21:1951-1961.
33. Quy PN, Kanai M, Fukuyama K, et al. Association between preanalytical factors and tumor mutational burden estimated by next-generation sequencing-based multiplex gene panel assay. [Internet].

Oncologist. 2019;24. https://pubmed.ncbi.nlm.nih.gov/31186376/. Accessed October 2, 2020.
34. Losic B, Craig AJ, Villacorta-Martin C, et al. Intratumoral heterogeneity and clonal evolution in liver cancer. [Internet]. *Nat Commun*. 2020;11:1-15. https://doi.org/10.1038/s41467-019-14050-z

SUPPORTING INFORMATION

Additional supporting information may be found online in the Supporting Information section.

How to cite this article: Wong CN, Fessas P, Dominy K, et al. Qualification of tumour mutational burden by targeted next-generation sequencing as a biomarker in hepatocellular carcinoma. *Liver Int*. 2020;00:1–12. https://doi.org/10.1111/liv.14706